The Etching Mechanism of $(Zr_{0.8}Sn_{0.2})TiO_4$(ZST) Film by Using Cl_2/O_2-Gas Plasma

K. -H. Kwon

Department of Electronic Engineering, Hanseo University, Seosan 356-820

A. M. Efremov

Dept. Microelectronic Devices and Materials Techology,
Ivanovo State University of Chemistry and Technology, F. Engels st., 7, 153460, Ivanovo, Russia

G. -Y. Yeom

Department of Materials Engineering, Sungkyunkwan University, Suwon 440-746

Y. I. Kang

Wireless Communication Devices Department of Basic Research Laboratory,
Electronics and Telecommunications Research Institute, Daejon 305-350

We investigated the etching mechanism of $(Zr_{0.8}Sn_{0.2})TiO_4$ film by using Cl_2/O_2-gas plasma. To understand the etching mechanism and etching rate behavior from the point of view of internal plasma properties and active particle kinetics, we used the plasma modeling. The data of Langmuir probe measurements and optical emission spectroscopy were used both as input data and model verification parameters etc. We also extracted the etching characteristics of the ZST film such as etch rate and analyzed the surface reaction by using XPS with various Cl_2/O_2-gas mixing ratios. On the basis of plasma modeling and experimental data, we will discuss the mechanism of ZST film etching in detail.

I. INTRODUCTION

There is currently an explosive growth in need for, and applications of, microwave circuit technologies. The progress in microwave communication applications and continuing miniaturization of integrated circuitry has resulted in demand for smaller microwave resonators, which are a key component in microwave circuits [1]. For developing thin film resonators, the complex perovskite material, Zirconium Tin Titanate (ZST), attracts an increasing interest due to its excellent microwave properties such as high dielectric constant ε_r, extremely low dielectric loss (high Q), and small temperature coefficient of resonator frequency. For fabricating ZST film resonator, the development of $(Zr_{0.8}Sn_{0.2})TiO_4$(ZST) etching technology is essential. Unfortunately, ZST etching has been scarcely investigated until now.

In this work, inductively coupled plasma (ICP) was used to investigate the etching technology of ZST films. Plasma processes utilizing ICP have been widely used as a promising technique to meet the increasingly stringent requirements in microelectronics fabrication. The high plasma density produced by ICP sources make them particularly attractive for applications. Some advantages in using this technique for etching include higher etch rate and lower ion bombardment energies compared to conventional reactive ion etching (RIE). Meanwhile, for etching perovskite materials Cl_2/O_2-gas chemistries are widely used in microelectronic technology [2,3].

However, achieving a desirable pattern requires solid understanding of etch behavior under various plasma discharge conditions. We used the plasma modeling to understand the behavior of etch mechanism and etch rate from the point of view of internal plasma properties and active particle kinetics.

At the same time, we also extracted the etching characteristics of the ZST film such as etch rate and analyzed the surface reaction by using XPS with various Cl_2/O_2-gas mixing ratios. ZST etch rate was also extracted by using scanning electron microscope (SEM).

We discussed the mechanism of ZST film etching on the basis of plasma modeling and experimental data.

II. EXPERIMENTAL PROCEDURE

Thin films of ZST were prepared by metal-organic solution deposition (MOSD) technique [4]. MOSD processing has been extensively used in thin film formation [5,6] because of the following advantages: easy composition control, good homogeneity and uniform deposition over a large substrate area [7]. Thin films of ZST were fabricated using zirconium(Zr) propoxide, tin(Sn)-isopropoxide and titanium(Ti)-isopropoxide as precursors. 2-methoxyethanol was selected as the solvent. The viscosity of the solution was controlled by varying the 2-methoxyethanol content. The precursor films were coated on Pt-sputtered Si substrates by spin coating technique at 2500 rpm for 30 seconds. After spin-coating on various substrates, films were baked in air on hot plate at 350 ° for 10 minutes. This step was repeated after each coating to ensure complete removal of volatile matter. The final thickness of the ZST films in this study was approximately 140 nm.

Plasma etching of this work was carried out using a homemade ICP etching system [2]. The top inductive coil was mounted on the quartz plate and connected to a RF power generator. The bottom electrode was connected to an RF (13.56 MHz) power generator through a matching box. The Cl_2/O_2-gas mixture was used and the total gas flow was kept at 30 sccm. The $O_2/(O_2 + Cl_2)$ mixing ratio was changed from 0 to 0.2. ICP source power, chamber pressure, and bias voltage were constant at 700 watts, 10mTorr, and –200 volts, respectively.

Results of plasma modeling were confirmed by using single Langmuir probe and optical emission spectroscopy (OES). The peaks due to emission by particular atoms or molecules were obtained by subtracting the background spectra due to stray light and detector noise. Electron energy distribution function (EEDF) was evaluated on the base of Langmuir probe measurements as a normalized second derivative of electron current branch. Relative volume concentrations of such plasma species as Cl, Cl_2 and O were measured at the characteristic emission line of 725.6 nm, 256 nm, 777.2 nm, respectively [8].
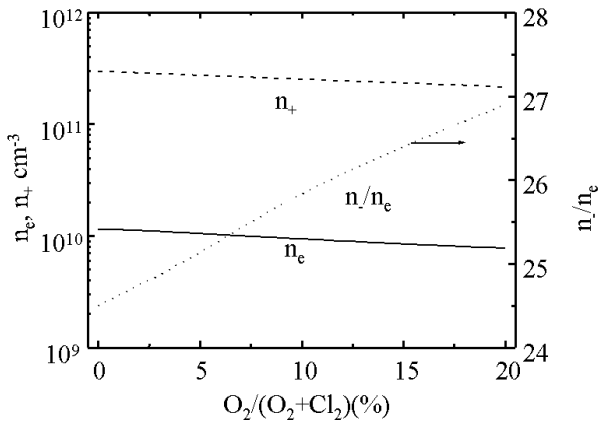
To investigate the etching characteristics, such as the etch rate, Hitachi SEM was used. The etch rate was extracted by measuring the film thickness difference before and after etching ZST film.

Compositional analysis of the ZST surface was performed using a VG Scientific ESCALAB 200R XPS (X-ray photoelectron spectroscopy) with Al Kα (1486.6 eV) radiation operating at 260 W. Narrow scan spectra of all regions of interest were recorded with 20 eV pass energy to quantify the surface composition and identify the chemical binding states.

III. RESULTS AND DISCUSSION

1. Plasma modeling

Ion bombardments and surface reactions have a large influence on the plasma etching characteristics. In this study, bias voltage was kept constant at −200 volts. Accordingly, ion and radical densities with various gas mixtures were modeled to investigate the influence of input parameters on the plasma etching characteristics. In this previous report, the procedure and assumptions of plasma modeling were described in detail [9].

Plasma modeling algorithm based on a simplest scheme to estimate relationships between input process parameters and final etching characteristics involving four main subsystems: 1) electron gas subsystem, 2) neutral particles subsystem, 3) charged particles subsystem, 4) heterogeneous processes subsystem. First subsystem based on the Boltzmann kinetic equation and a heat transfer equation. Second and third subsystems are described by chemical kinetics and transport equations. Fourth subsystem based on heterogeneous chemistry. The data of Langmuir probe measurements and OES were used both as input data and model verification parameters.

Fig. 1 illustrates modeling results concerning the influence of Cl_2/O_2-mixing content on volume densities of electrons, positive ions and relative density of negative ions, which was determined as n_-/n_e. It is evident that addition of oxygen in plasma mixture leads to weak decreasing of both electrons and positive ions volume densities. Meanwhile, we also found out from Langmuir probe experiment that oxygen addition leaded to the decrease in electron saturation current. This implies that the modeling results of electron density are in good agreement with experimental data. To obtain the charged particle densities, we considered the formation and decay processes of the charged particles. We also found out from calculations that the addition of O_2 leaded to the increase in total ionization due to the increase in ionization rate. Similar results were reported in previous report [10]. In low-pressure discharges such as this ICP system electron decay is dominantly controlled by
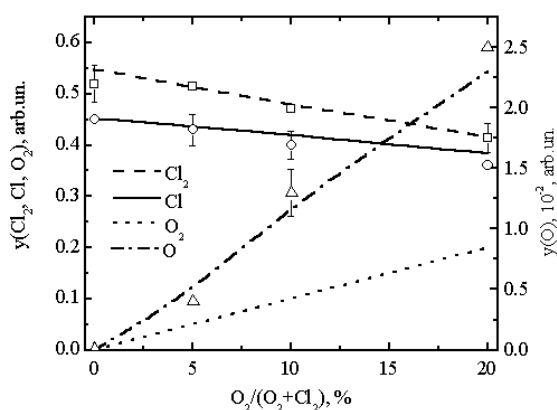

Fig. 1. The influence of Cl_2/O_2 mixing on volume densities of electrons, positive ions and relative density of negative ions.

Fig. 2. Relative fractions of neutral particles in Cl_2/O_2 mixture. Points represent normalized emission intensities of Cl_2, Cl and O.

diffusion. Accordingly, electron volume density is determined by correlation between electron impact ionization and electron diffusion. The comparison between rates of electron formation and decay processes showed that increasing of oxygen content in the plasma leaded to the increase in both ionization and diffusion decay rate of electrons. At the same time diffusion rate increased more rapidly, which caused the decrease of electron volume density. The same arguments may be applied for the explanation of the volume density behavior of positive ions.

Fig 2 shows the relative fractions of neutral particles in Cl_2/O_2 mixture. Points represent the normalized emission intensities of Cl_2, Cl and O. Points correspond to experimental data concerning normalized relative emission intensities of Cl_2 (256 nm), Cl (725.6 nm), O (777.2 nm) measured by OES. Under the low-pressure discharge conditions, the balance of neutral particles is determined by the correlation between direct electron impact dissociation and heterogeneous decay on chamber walls sup-
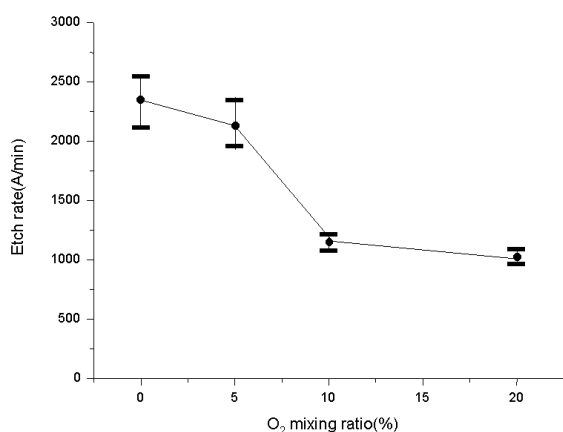
ported by diffusion. The behavior of volume densities of atoms and molecules should be mainly determined by variations of both initial mixture and the rates of volume generation processes, such as electron impact dissociation. This figure showed that additive oxygen leaded to the monotonous decrease of volume densities of chlorine molecules and atoms while densities of O_2 and O atoms increased proportionally with oxygen content in initial mixture. It is important to note that chlorine and oxygen molecules are characterized by different amount of dissociation. Mean dissociation percentage for Cl_2 molecules are about 45 % while a corresponding value for O_2 do not exceeds 10 %. Low dissociation percentage of molecular oxygen and thus relatively low volume density of oxygen atoms may be explained, except initial mixture composition, by higher dissociation threshold of O_2 in comparison with chlorine molecules (6.1 eV and 3.4 eV, respectively).

2. Etch rate of ZST films

The etching rate of ZST films using Cl_2/O_2-gas plasma (Fig. 3) was investigated. This figure shows that the etching rate rapidly decreased at O_2-gas mixing ratio of 5 % and was kept nearly constant over this ratio. Up to the ratio of 5 %, etch rates decreased with increasing O_2 ratios. In this region, since the bias potential was fixed ($-$ 200 V), the change of etch rates can be explained by etching species(that is, radicals and ions) generated at the plasma. That is, in Fig. 1 and 2, addition of O_2-gas showed the decrease of positive ion densities and Cl radical density and the increase of O radicals in the plasma. As a result, up to the ratio of 5 %, etch rates decreased with increasing O_2 ratios. At the same time, compared to pure Cl_2 plasma, the densities of positive ions and Cl radicals monotonously decreased up to the ratio of 20 %. However, etch rates rapidly decreased over the ratio of 5 % and was saturated. This implies that another factor such as O radical change in addition to the change of ion and radical densities relates to the change of etch rates.

Fig. 3. The etching rate of ZST films using Cl_2/O_2-gas plasma.

3. Surface reaction

To investigate the surface reaction on the ZST films, XPS analysis was carried out. The primary elements detected by the wide scan analysis of XPS were Zr, Sn, Ti, O, Cl and C.

Figure 4 presents the changes of elemental compositions on samples etched in various Cl_2/O_2-gas mixing ratio (O_2 flow rate / total gas flow rate). In the case of C, it was detected due to air contamination. Accordingly, C content was excluded for calculating atomic contents of composed elements. Meanwhile, the atomic content of
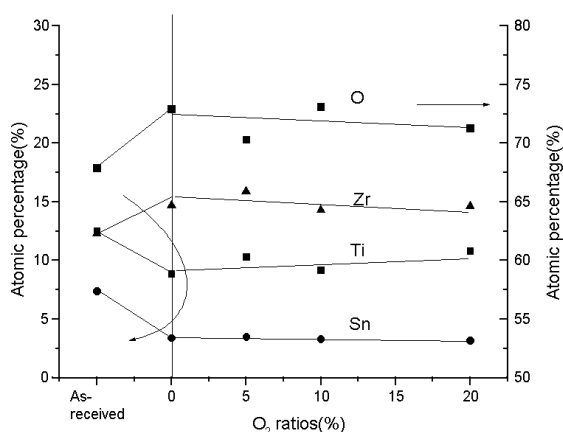
Fig. 4. The changes of element compositions on samples etched in various Cl_2/O_2-gas mixing ratio (O_2 flow rate / total gas flow rate).

Fig. 6. Ti 2p narrow scan spectra with various gas ratios.

Cl was also detected less than 2 % and the variation of its atomic % was less than 1 and its peak profile was little changes. So, we could not get any useful information from Cl 2p spectra. At the same time, it is important to know relative changes of composed elements before and after Cl_2/O_2 plasma exposure. Accordingly, in this calculation of atomic contents, Cl element was also excluded.

Compared constituent elements on an as-received sample to those on a sample etched by pure Cl_2 gas, the content of Zr element increased but those of Ti and Sn decreased. This result indicates that while Ti and Sn were easily removed by Cl_2-gas plasma, the removing rate of Zr was slower than that of Ti and Sn. This phenomenon can be explained by the difference of vapor pressure of each chlorine compounds. The vapor pressures of $ZrCl_4$, $SnCl_4$, and $TiCl_4$ are 190 ^oC, -22.7 ^oC, and –13.9^oC for 1 mmHg, respectively [8]. That is, while $SnCl_4$ and $TiCl_4$ formed by Cl_2-gas plasma on the etched surface could easily evaporate due to those high
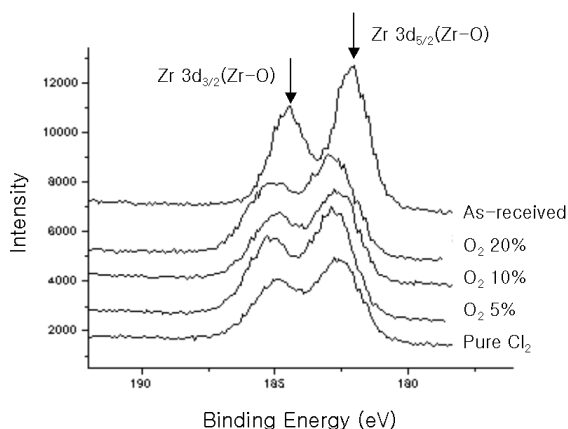
vapor pressures, $ZrCl_4$ could hardly evaporate due to its low vapor pressure. At the same time, contents of Zr and Sn are scarcely changed, while the atomic content of Ti increases with increasing Cl_2/O_2 -gas mixing ratio.

To investigate the cause of the change of atomic contents on the etched surface with varying gas-mixing ratio, the narrow scan spectra of each element were examined.

Zr 3d spectra of samples etched in various gas-mixing ratios are plotted in Fig. 5. It is well known that narrow scan spectra of Zr 3d have two peaks which correspond to Zr $3d_{5/2}$ and Zr $3d_{3/2}$, respectively. In this figure, we can also find out two peaks at the binding energies of 182.1 and 184.4 eV. These peaks typically correspond to Zr 3d binding energies of Zr-O [11]. At the same time, Zr $3d_{5/2}$ peak on the pure Cl_2 etched sample was detected at the binding energy of 182.7 eV. Comparing with the binding energy of the as-received sample, we find the peak shift to higher binding energy by Cl_2-gas etching. Accordingly, the shift of the binding energy could be explained that it resulted from chlorinated $ZrO_x(x \le 2)$.

Figure 6 shows the Ti 2p narrow scan spectra with the ratios. In general, the peak of elementary Ti 2p is composed of two peaks of Ti $2p_{3/2}$ and Ti $2p_{1/2}$ detected at the binding energies of 454.1 eV and 460.2 eV, respectively. In the case of the as-received sample, the peak of Ti $2p_{3/2}$ was observed at the binding energy of 458.4 eV. Considering that Ti $2p_{3/2}$ peaks from TiO and TiO_2 were generally observed at the binding energy of 455.1 and 458.8 eV, respectively, the peak detected at the binding energy of 458.4 eV was thought to be from $TiO_x(x \le 2)$ compounds. At the same time, in the case of the pure Cl etched samples, the peak of Ti 2p was detected at the binding energy of 459 eV. It is thought that this peak shift was induced from Cl incorporation to $TiO_x(x \le 2)$ which could form metal chlorate(metal-Cl_xO_y) compounds. Meanwhile, it was found that the peak height induced from metal chlorates increased with increasing O_2 addition. This phenomenon can be explained by Fig. 2. In Fig. 2, O radical density was increased and Cl was a little decreased. Accordingly, O radicals increased with increasing O_2 ratios react to Ti

Fig. 5. Zr 3d spectra of samples etched in various gas-mixing ratios.

to prevent the formation of volatile compounds such as $TiCl_4$. Accordingly, the increase of O_2 ratio increases the amount of Ti on the etched surface. As a result, etch rates rapidly decreased over the O_2 ratio of 5 %.

IV. CONCLUSION

We investigated the etching mechanism of $(Zr_{0.8}Sn_{0.2})TiO_4$ film by using Cl_2/O_2-gas plasma. To understand the etching mechanism and etching rate behavior from the point of view of internal plasma properties and active particle kinetics, we used the plasma modeling. Modeling results showed that the positive ion density decreased with increasing O_2 ratios. At the same time, It was also found that Cl radical density decreased, while O radical density increased with increasing O_2 ratios. Meanwhile, the etch rate of ZST film rapidly decreased at O_2 ratios of 5 %. From these results, the decrease of the ZST etch rate could result from decreasing positive ion density and Cl radical density and increasing O radical density of the etched surface. At the same time, from XPS analysis, we also found that the atomic content of Ti increased with increasing O_2 ratios. This means that among constituent elements, Ti has a large influence on the decrease of ZST etch rates by O_2 addition to Cl_2 plasma.

REFERENCES

[1] A. J. Moulson and J. M. Herbert, *Electroceramics* (Chapman and Hall, New York, 1990)
[2] K.-H. Kwon, S.-Y. Kang, S.-K. Lee, S.-I. Kim, N.-K. Hong, S. Nahm and Y.-S. Kim, Journal of The Electrochemical Society **149**, C280 (2002).
[3] K.-H. Kwon, S.-Y. Kang, G.-Y. Yeom, N.-K. Hong and J. H. Lee, Journal of The Electrochemical Society **147**, 1807 (2000).
[4] D. W. Lee, S. Nahm, M.H. Kim and J. D. Byun, The Korean Journal of Ceramics **2**, 162 (1996).
[5] P. C. Joshi and S. B. Desu, Applied Physics Letters **73**, 1080 (1998).
[6] M. A. Salam, H. Konishi, M. Mizuno, H. Fukuda and S. Nomura, Jpn. J. Appl. Phys. **40** Part 1. No. 3A., 1431 (2001).
[7] D. Meyerhofer, J. Appl. Phys. **49**, 3993 (1978).
[8] D. R. Lide(Ed) *Handbook of Chemistry and Physics*, 76th edition (CRC press, 1995).
[9] D. P. Kim, C. I. Kim, K.-H. Kwon, A. Efremov and G. Y. Yeom, Plasma source science and technology, submitted
[10] B. S. Danilin and V. J. Kireev, *The Applications of Low Temperature Plasma for a Materials Etching and Cleaninig* ("Energoatomizdat" edition, Moscow, 1987), p.263 (in Russian)
[11] F. Moulder, W. F. Stickle, P. E. Sobol and K. D. Bomben (Eds.) *Handbook of X-ray Photoelectron Spectroscopy* (Physical Electronics Inc., 1995), p.108.